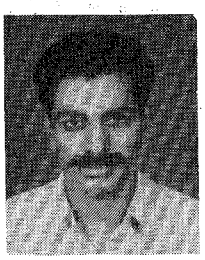

of Electrical Engineering, Indian Institute of Technology, Kanpur, India, working as a Research Engineer in the area of computer-aided analysis and design of microwave integrated circuits. Presently, he is with the Department of Electrical Engineering, University of Waterloo, Waterloo, Ontario, Canada, working in the area of optimization for large networks. He has published ten research papers and is a co-author of the book *Computer-Aided Design of Microwave Circuits*, Artech House, 1981.

✚

K. C. Gupta (M'62–SM'74) was born in 1940. He received the B.E. and M.E. degrees in electrical communication engineering from Indian Institute of Science, Bangalore, India, in 1961 and 1962, respectively, and the Ph.D. degree from Birla Institute of Technology and Science, Pilani, India, in 1969.

He worked at Punjab Engineering College, Chandigarh, India, from 1964 to 1965, the Central Electronics Engineering Research Institute, Pilani, India, from 1965 to 1968, and Birla Institute of Technology from 1968 to 1969. Since 1969 he has been with the Indian Institute of Technology, Kanpur, India, and has been a Professor of electrical engineering since 1975. On leave from the Indian Institute of Technology, he was a Visiting Professor at the University of Waterloo, Canada from 1975 to 1976, Ecole Polytechnique Federale de Lausanne, Switzerland, in 1976, Technical University of Denmark from 1976 to 1977, and Eidgenossische Technische Hochschule, Zurich, Switzerland, in 1979. From 1971 to 1979 he was Coordinator for the Phased Array Radar Group of Advanced Centre for Electronic Systems at the Indian Institute of Technology. He has published four books: *Microwave Integrated Circuits*, Wiley Eastern and Halsted Press, 1974, *Microstrip Lines and Slotlines*, Artech House, 1979, *Microwaves*, Wiley Eastern, 1979 Halsted Press, 1980, and *Computer-Aided Design of Microwave Circuits*, Artech House, 1981. He has published over 70 research papers and holds one patent in microwaves areas.

Dr. Gupta is a fellow of the Institution of Electronics and Telecommunication Engineers (India).

Millimeter-Wave Hybrid Coupled Reflection Amplifiers and Multiplexers

DAVID RUBIN, MEMBER, IEEE

Abstract—**Multiple stage hybrid coupled reflection amplifiers and frequency multipliers are modeled using two-port analysis. A two-stage (4 diode) microstrip InP Gunn amplifier and a four-section suspended substrate multiplexer were fabricated in *Ka* band. Analysis shows that the performance of the hybrid coupled amplifier, both for packaged diodes and pure negative resistance (ideal monolithic) devices, is extremely sensitive to input and output VSWR's.**

I. Introduction

THE 3-dB QUADRATURE coupler is one of the most useful microwave components available to the circuit designer. The amplifier and multiplexer configurations to be described both use the equal power split and 90° phase differences between output terminals of these "hybrids". Symmetry makes it possible to reduce the analysis of the four-port network to that of a two-port. Identical terminations present no problems since they do not upset symmetry and can be considered part of the coupler for analysis purposes. Nonidentical terminations, such as two different diodes, can be handled by signal flow graphs, again reducing the circuit to an equivalent two-port.

This paper describes the analysis of complex microwave circuits which utilize 3-dB quadrature couplers. Both computer results and measurements will be given for: 1) single and multistage hybrid coupled small signal reflection amplifiers, and 2) multichannel hybrid coupled multiplexers.

Predicted behavior of ideal negative resistance devices is also computed for circuits which utilize different practical hybrid couplers and mismatched input and output impedances. It will be shown that small mismatches can lead to large amplitude ripple and input VSWR.

II. Analysis of Cascaded Hybrid Coupled Reflection Amplifiers

All solid-state amplifiers for use above 40 GHz use negative resistance one-port devices as amplifying elements. To separate input and output power, ferrite circulators are normally used. At the higher millimeter-wave frequencies, circulators are bandwidth limited; another technique, that of coupling two identical amplifier stages through 3-dB quadrature couplers, is sometimes used [1]. This method makes use of the fact that the two output

Manuscript received March 16, 1982; revised June 18, 1982.

The author is with Millimeter-Wave Technology Branch, Naval Ocean Systems Center, San Diego, CA 92152.

0018-9480/82/1200-2156$00.75 ©1982 IEEE

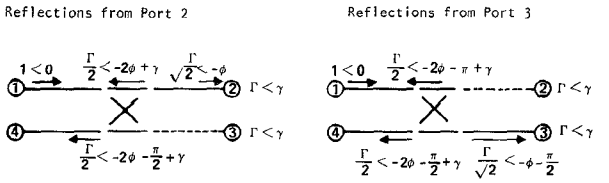

Fig. 1. Ideal 3-dB quadrature coupler.

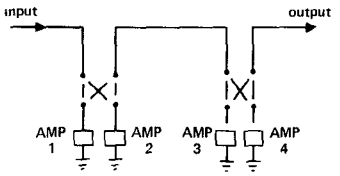

Fig. 2. Cascaded hybrid-coupled amplifiers.

ports of these couplers are close to 90° out of phase over large frequency ranges. Fig. 1 illustrates schematically, through voltage superposition, the additive phasing of the two reflected waves (at port 4) and the absence of any reflected wave at the input (port 1). A transversal of RF through the coupler in the horizontal direction suffers the phase shift $-\phi°$, and through the diagonal direction an additional shift of $-90°$.

Only if the couplers are ideal and if both amplifiers have the same reflection coefficient will all of the amplified power be available at port 4. Fig. 2 illustrates how two such stages can be cascaded. Further extensions of ideal couplers and amplifiers are obvious.

There are many nonideal elements in practical amplifiers, particularly in microstrip, which tend to couple output power back to the input port, providing nonuniform gain and limiting bandwidth. These include 1) nonideal couplers (poor directivity, input VSWR, and/or power split, 2) nonideal amplifiers (different diode characteristics), and 3) nonideal transitions (poor VSWR going from waveguide to microstrip).

The problems of nonideal elements are so complex that a computer must be used to determine the likely sources of error. When two hybrid coupled amplifiers were cascaded together, the author found little correlation to what was expected using ideal models. Computer routines were then written which incorporated hybrid coupler models with actual amplifier stages (even for different diodes), connecting lines between the amplifiers, and microstrip transition VSWR's at the input and output of the cascaded amplifiers.

III. Description of Programs

A. Symmetric Four-Port

Two-port analysis can easily be extended to provide input and output parameters of symmetric four-ports using superposition of even and odd modes. Hybrid coupled identical amplifier stages can be calculated using two-port analysis as shown in Fig. 3.

The reflection coefficient

$$b_1/a_1 = (1/2)S_{11'e} + (1/2)S_{11'0} \qquad (1)$$

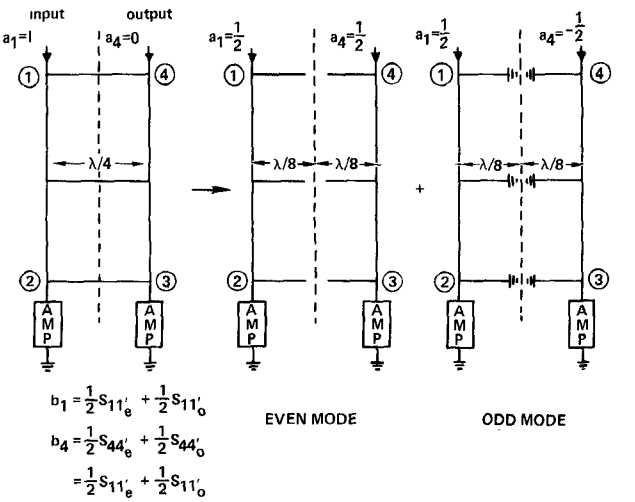

Fig. 3. Even- and odd-mode hybrid coupled amplifier analysis.

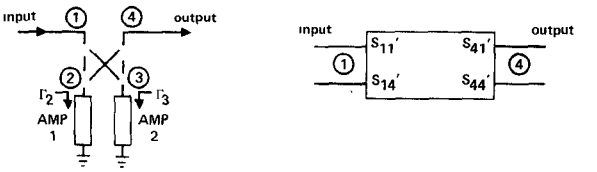

Fig. 4. Nonidentical reflection amplifier stages combined to form two-port.

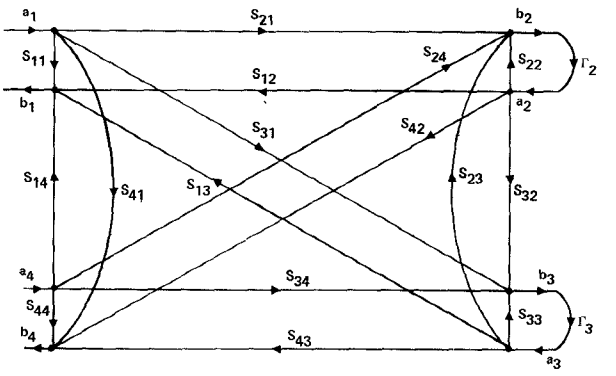

Fig. 5. Flow graph of amplifier in Fig. 4.

and the voltage gain

$$b_4/a_1 = (1/2)S_{11'e} - (1/2)S_{11'o} \qquad (2)$$

where $S_{11'e}$ and $S_{11'o}$ are the input reflection coefficients calculated from the even- and odd-mode circuits of Fig. 3(b) and 3(c), respectively.

B. Unsymmetrically Loaded Symmetric Four-Ports

Suppose the symmetric hybrid couplers were loaded with diodes which were somewhat different. Two-port analysis can again be used to convert unsymmetrically loaded symmetric four-ports as in Fig. 4(a) and 4(b); however, a few intermediate steps must be used. Fig. 5 is a flow graph representation of any four-port with output terminals connected to any two loads (such as amplifiers) with reflection coefficients Γ_2 and Γ_3.

The solution to the flow graph problem (i.e., what is $b_4/a_1, b_1/a_1$) can most easily be found using Mason's

rules for loop analysis [3]. Keeping track of all loops, the transmission path (scattering parameter) from between any input and output port is given by

$$T=\frac{\begin{array}{l}P_1\left(1-L(1)^{(1)}+L(2)^{(1)}-\cdots\right)\\ +P_2\left(1-L(1)^{(2)}+L(2)^{(2)}-\cdots\right)+\cdots\end{array}}{1-L(1)+L(2)-L(3)+\cdots} \tag{3}$$

where $P_1, P_2, \cdots$ are different transmission paths between ports, $L(1)$ is any single loop, $L(2)$ is any two nontouching loops multiplied together, $L(3)$ is any three nontouching loops multiplied together, etc. $L(1)^{(1)}$ is any nontouching loop that does not touch the path P_1, etc.

An example of one path from the input to the output port 1 (reflection) is S_{11}. Another path is $S_{31}\cdot\Gamma_3\cdot S_{23}\cdot\Gamma_2\cdot S_{12}$. A simple first-order loop is $\Gamma_2\cdot S_{22}$. One second-order loop is $\Gamma_2\cdot S_{22}\cdot\Gamma_3\cdot S_{33}$.

Mason's rule therefore gives for voltage gain

$$\frac{b_4}{a_1}=S_{41}'=S_{14}+\frac{\begin{array}{l}S_{21}\Gamma_2S_{24}(1-\Gamma_3S_{11})+S_{31}\Gamma_3S_{34}(1-\Gamma_2S_{22})\\ +S_{21}\Gamma_2S_{32}\Gamma_3S_{34}+S_{31}\Gamma_3S_{23}\Gamma_2S_{24}\end{array}}{\begin{array}{c}1-(\Gamma_2S_{22}+\Gamma_3S_{33}+S_{23}S_{32}\Gamma_2\Gamma_3)\\ +S_{22}\Gamma_2S_{33}\Gamma_3\end{array}}.$$

For symmetric four-ports (such as hybrid couplers) $S_{22}=S_{33}=S_{11}, S_{31}=S_{24}=S_{13}, S_{23}=S_{32}=S_{14}$. Calling the denominator L

$$L=1-S_{11}(\Gamma_2+\Gamma_3)+\Gamma_2\Gamma_3\left(S_{11}^2-S_{14}^2\right) \tag{4}$$

then

$$S_{41}'=S_{14}+\frac{1}{L}\{S_{12}S_{13}\Gamma_2(1-\Gamma_3S_{11})+S_{13}S_{12}\Gamma_3(1-\Gamma_2S_{11})+\Gamma_2\Gamma_3S_{14}\left(S_{12}^2+S_{13}^2\right)\}. \tag{5}$$

Likewise for return loss (or gain)

$$b_1/a_1=S_{11}'=S_{11}+1/L\{S_{21}\Gamma_2S_{12}(1-S_{33}\Gamma_3)+S_{31}\Gamma_3S_{13}(1-S_{22}\Gamma_2)+S_{21}\Gamma_2S_{32}\Gamma_3S_{13}+S_{31}\Gamma_3S_{23}\Gamma_2S_{12}\}$$

which reduces to

$$S_{11}'=S_{11}+\frac{1}{L}\{S_{12}{}^2\Gamma_2(1-S_{11}\Gamma_3)+S_{13}{}^2\Gamma_3(1-S_{11}\Gamma_2)+2\Gamma_2\Gamma_3S_{12}S_{13}S_{14}\}. \tag{6}$$

Whether or not $\Gamma_2=\Gamma_3$, $S_{14}'=S_{41}'$, however

$$b_4/a_4=S_{44}'=S_{11}+\frac{1}{L}\{S_{12}{}^2\Gamma_3(1-S_{11}\Gamma_2)+S_{13}{}^2\Gamma_2(1-S_{11}\Gamma_3)+2\Gamma_2\Gamma_3S_{12}S_{13}S_{14}\} \tag{7}$$

which is not equal to S_{11}' unless $\Gamma_2=\Gamma_3$, i.e., unless there is complete symmetry.

The resultant two-port, represented by parameters S_{11}', S_{14}', S_{41}', and S_{44}', can be converted to $ABCD$ matrix form and used in a subsequent two-port analysis.

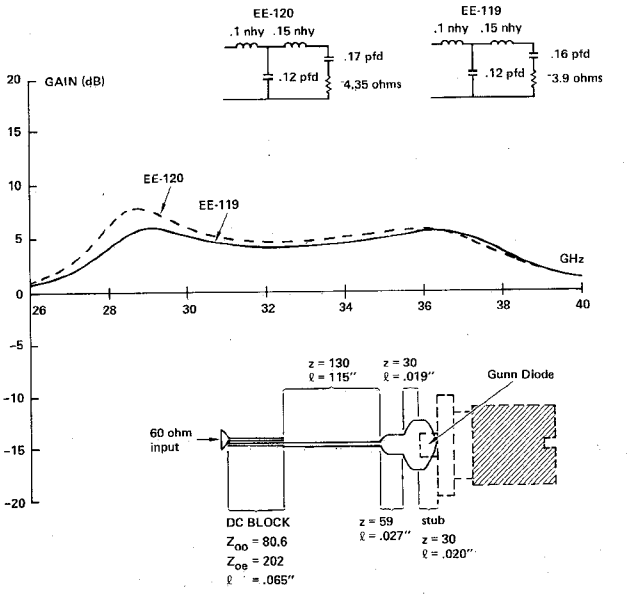

Fig. 6. Wide-band matching network and computed reflection gain for two different diodes.

IV. Computation of Cascaded Hybrid Coupled Amplifier Parameters

All calculations to be presented have been performed on a Textronix 4052 minicomputer using BASIC language programming. Internal magnetic tape files are used to store S parameters of various hybrids and reflection coefficients calculated from a number of amplifier stages over 26–40 GHz in 0.2-GHz increments. The calculating routine brings up any of the desired stored parameters in the proper sequence for network analysis. The effects of transition VSWR's can be simulated by reactively shunting the input and output lines at the proper distances. The results take about two minutes for a two-stage amplifier and allow a fast look at the differences encountered when particular amplifier matching networks are used with various couplers, interstage transmission line lengths, and waveguide to microstrip transition VSWR's.

The diode models were determined by Varian from small signal reflection gain in coaxial cavities [4]. The design of single-stage reflection amplifiers has previously been outlined [5]. Fig. 6 details the parameters and computed performance of two different diodes in a wide-band matching circuit. All computations use input and output transmission lines of $Z_0=60\ \Omega$, corresponding to our best transition match, and 2.2-dielectric constant microstrip. The synchronous coupler parameters of Fig. 7 are based on a 4-dB Chebyschev design by Levy [6] with modified end branch lines. The amplifier configurations of Fig. 8 utilize the above components with appropriate interconnecting 60-Ω line lengths. No transition mismatch is used at the input and output of these computer models.

Fig. 8(a) shows the gain and return loss of a single-stage hybrid coupled amplifier using two EE-119 diodes. Fig. 8(b) shows the gain and return loss of the same amplifier using slightly different diodes (one EE-119 and one EE-120). Fig. 8(c) shows the gain and return loss of a two-stage hybrid coupled amplifier with all four identical diodes (EE-119's).

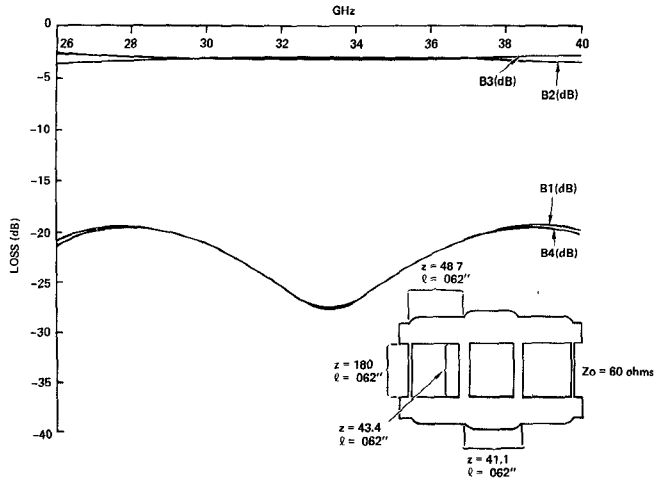

Fig. 7. Computed performance of modified 4-branch synchronous coupler.

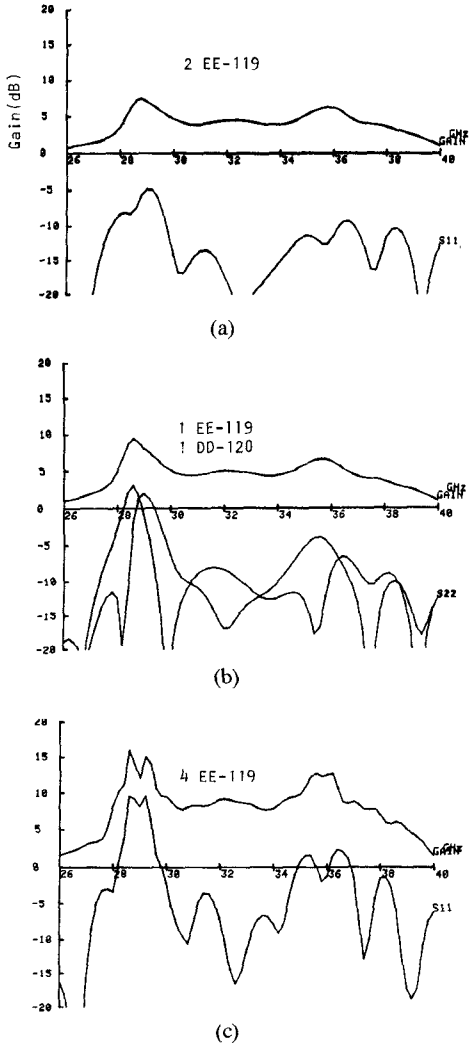

Fig. 8. Computed performance of one- and two-stage amplifier using elements of Figs. 6 and 7. (a) Single stage–identical diodes. (b) Single stage–different diodes. (c) Two stages–identical diodes.

A circuit based on the computer model which gave Fig. 8(c) is shown in Fig. 9 along with measured results. It is likely, as will be shown, that differences between measured and computed results can be attributed to transition VSWR's which were not accounted for in the above models.

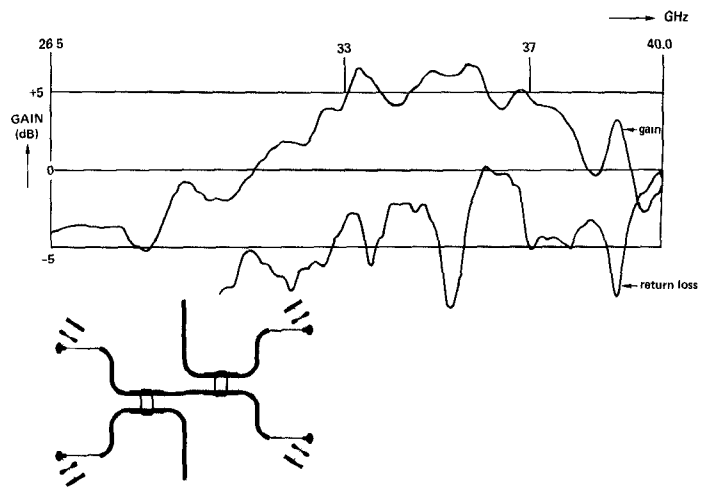

Fig. 9. Measured performance and circuit pattern of two-stage amplifier based on the model of Fig. 8(c).

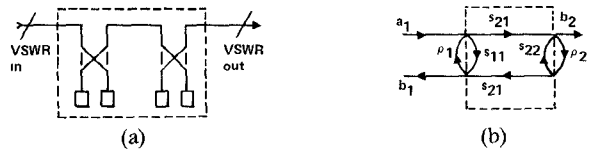

Fig. 10. (a) Two-port equivalent. (b) Flow graph.

V. The VSWR Problem

Unlike transistor amplifiers which have some degree of internal isolation, i.e., $S_{12} \ll S_{21}$, either end of a hybrid coupled reflection amplifier can be used as the input. Any reflections from the load terminal are reflected back toward the input with gain. If the generator is not perfectly matched an additional reflection is caused at the input. Knowing the two-port parameters of the reflection amplifier and the load and input reflection coefficients allows a calculation of the total circuit gain and return loss.

Any single- or multiple-stage reflection amplifier can be reduced to a two-port with input and output shown in Fig. 10(a). A flow graph comprising both amplifier and input and output reflection coefficients (due to transitions, mismatched impedances, etc.) is shown in Fig. 10(b).

Without additional VSWR at the input and output terminals the power gain would be

$$\left|\frac{b_2}{a_1}\right|^2 = \left|\frac{S_{21}}{1-(\rho_1 S_{11}+\rho_2 S_{22}+\rho_1\rho_2 S_{21}^2)+\rho_1\rho_2 S_{11}S_{12}}\right|^2 \tag{8}$$

and return loss

$$\left|\frac{b_1}{a_1}\right|^2 = \left|\frac{S_{11}(1-\rho_2 S_{22})+S_{21}{}^2\rho_2}{1-(\rho_1 S_{11}+\rho_2 S_{22}+\rho_1\rho_2 S_{21}^2)+\rho_1\rho_2 S_{11}S_{22}}\right|^2. \tag{9}$$

The worst-case effects of the VSWR's associated with transitions or terminations can be found by assigning phases to the parameters of (8) and (9). Table I lists the maximum gain variations (CHG DB) associated with external input and output reflections (ρ_1 and ρ_2) for amplifiers with 5- and 10-dB gain and equal values of S_{11} and S_{22}.

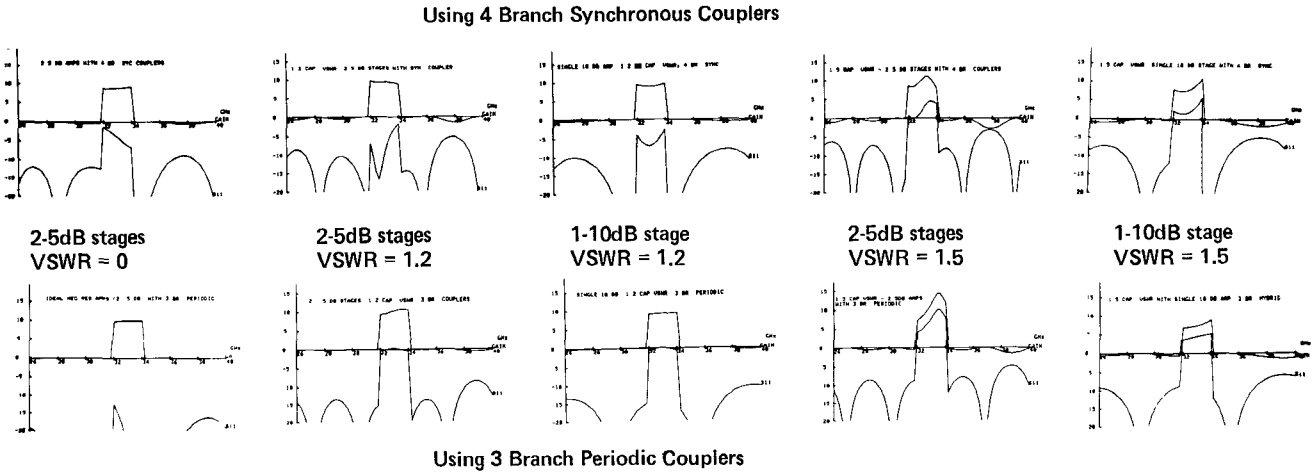

Fig. 11. 10-dB gain hybrid coupled amplifiers (one and two stages) using ideal negative resistance amplifying elements between 32 and 34 GHz. Input and output VSWR's have been set equal and are capacitive.

TABLE I
DEGRADATION OF HYBRID COUPLED AMPLIFIER PERFORMANCE DUE TO EXTERNAL INPUT AND OUTPUT VSWR (REFLECTION RETURN LOSSES P_1 AND P_2)

GAIN(DB)	CHG(DB)	$S_{11}=S_{22}$(DB)	RET.LOSS	P_1(DB)	P_2(DB)
5.00	1.22	-10.00	-5.32	-20.00	-25.00
5.00	1.75	-10.00	-2.92	-20.00	-20.00
5.00	2.70	-10.00	0.58	-20.00	-15.00
5.00	4.43	-10.00	5.00	-20.00	-10.00
5.00	1.94	-10.00	-5.00	-15.00	-25.00
5.00	2.70	-10.00	-2.39	-15.00	-20.00
5.00	4.07	-10.00	1.32	-15.00	-15.00
5.00	6.66	-10.00	6.55	-15.00	-10.00
5.00	3.23	-10.00	-4.26	-10.00	-25.00
5.00	4.43	-10.00	-1.35	-10.00	-20.00
5.00	6.66	-10.00	3.00	-10.00	-15.00
5.00	11.31	-10.00	9.97	-10.00	-10.00
5.00	1.94	-5.00	-1.38	-20.00	-25.00
5.00	2.70	-5.00	0.64	-20.00	-20.00
5.00	4.07	-5.00	3.72	-20.00	-15.00
5.00	6.66	-5.00	8.37	-20.00	-10.00
5.00	3.04	-5.00	-0.75	-15.00	-25.00
5.00	4.07	-5.00	1.46	-15.00	-20.00
5.00	5.99	-5.00	4.94	-15.00	-15.00
5.00	9.82	-5.00	10.64	-15.00	-10.00
5.00	5.06	-5.00	0.49	-10.00	-25.00
5.00	6.66	-5.00	3.14	-10.00	-20.00
5.00	9.82	-5.00	7.67	-10.00	-15.00
5.00	17.01	-5.00	17.25	-10.00	-10.00

GAIN(DB)	CHG(DB)	$S_{11}=S_{22}$(DB)	RET.LOSS	P_1(DB)	P_2(DB)
10.00	1.94	-10.00	-8.04	-20.00	-25.00
10.00	3.04	-10.00	4.10	-20.00	-20.00
10.00	5.06	-10.00	9.39	-20.00	-15.00
10.00	9.87	-10.00	16.50	-20.00	-10.00
10.00	3.23	-10.00	0.70	-15.00	-25.00
10.00	5.06	-10.00	5.35	-15.00	-20.00
10.00	8.65	-10.00	11.85	-15.00	-15.00
10.00	17.93	-10.00	23.86	-15.00	-10.00
10.00	5.67	-10.00	2.20	-10.00	-25.00
10.00	9.87	-10.00	8.12	-10.00	-20.00
10.00	17.93	-10.00	19.44	-10.00	-15.00
10.00	17.69	-10.00	21.36	-10.00	-10.00
10.00	2.70	-5.00	2.61	-20.00	-25.00
10.00	4.07	-5.00	6.32	-20.00	-20.00
10.00	6.66	-5.00	11.55	-20.00	-15.00
10.00	12.22	-5.00	19.75	-20.00	-10.00
10.00	4.43	-5.00	3.65	-15.00	-25.00
10.00	6.66	-5.00	8.00	-15.00	-20.00
10.00	11.31	-5.00	14.97	-15.00	-15.00
10.00	30.22	-5.00	36.11	-15.00	-10.00
10.00	7.75	-5.00	5.87	-10.00	-25.00
10.00	12.22	-5.00	12.15	-10.00	-20.00
10.00	30.22	-5.00	32.05	-10.00	-15.00
10.00	13.53	-5.00	17.11	-10.00	-10.00

Extending the table to cover 15 dB showed no useful amplifiers with the given reflection conditions. Some conclusions: 1) The output transition/termination affects the return loss of the amplifier more than the input transition/termination; 2) 10-dB amplifiers require input and output VSWR's corresponding to -20-dB return loss or greater; and 3) 5-dB amplifier require input VSWR's corresponding to -15 dB or greater, and output VSWR's corresponding to -20 dB or greater.

The chart is probably too restrictive, since it accounts for phase changes corresponding to the worst case. The latter is only approached when the distances between circuit elements are in the order of one or more wavelengths. Fig. 11 is a composite of gain and return losses of single- and dual-stage amplifiers using "ideal" negative resistance diodes (no parasitics) and two different types of couplers. The four branch synchronous type has been used with our amplifiers because of its large bandwidth. The three branch periodic has nearly infinite return loss and directivity over a narrow band. The computer model is for pure negative resistance elements over a 2-GHz bandwidth (frequency center of coupler) and zero resistance outside of this frequency range. The circuit used is that of Figs. 8 and 9 except for zero transmission line lengths between the coupler outputs and the dc blocks. No matching elements are used with the ficticious diodes. The model should scale, i.e., the number of wavelengths between elements will remain constant with dielectric or semi-insulating substrates (monolithic amplifier).

1) Even for an ideal hybrid coupled amplifier, input and output VSWR's should be less than 1.2 (-20-dB return loss). In general, this may require very good isolators.

2) The limiting criteria for hybrid coupled amplifiers are not diode package-parasitics or low directivity couplers, but transition VSWR and load mismatch.

VI. MULTIPLEXER ANALYSIS

The circuit pattern of a four-channel suspended substrate multiplexer recently developed at NOSC [7] is shown in Fig. 12. The multiplexer routes RF input between 26 and 42 GHz into one of four output ports. Although the circuit is quite complex, it can easily be analyzed using two-port methods similar to that used for the hybrid coupled amplifiers. In this case it is necessary to find the bandpass characteristics for each of the output ports with respect to the input port.

Each of the four sections can be modeled as in Fig. 13, using its particular filter sections. The internal symmetric four-port can be handled as in Section III using even- and odd-mode analysis. The results would yield the four-port scattering parameters S_{ij}' where $S_{ij}' = S_{ij}'$. It is necessary to find, with respect to input voltage a_1, the output voltage b_3, the reflected voltage b_1, and the voltage to the succeeding port b_4. We will assume that the internal and

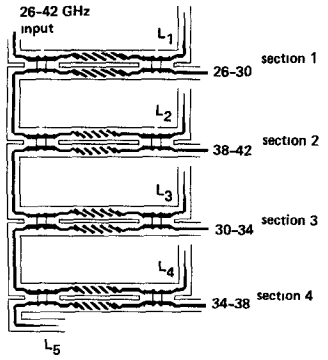

Fig. 12. Circuit pattern for 4-channel multiplexer.

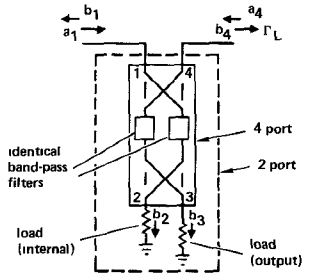

Fig. 13. Two-port for single section of multiplexer.

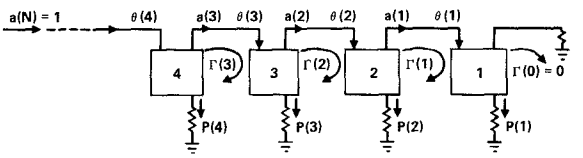

Fig. 14. Cascaded multiplexer sections.

external loads are perfect so that $a_2 = a_3 = 0$. From the 2-port: $b_4 = S_{41}'a_1 + S_{44}'a_4$, and since $a_4 = \Gamma_L b_4$

$$b_4 = \frac{S_{41}'a_1}{1-\Gamma_L S_{44}'} = \frac{S_{14}'a_1}{1-\Gamma_L S_{11}'}. \tag{10}$$

From the 4-port: $b_3 = S_{31}'a_1 + S_{34}'a_4$, and since $a_4 = \Gamma_L b_4$

$$|b_3|^2 = \left|S_{13}' + \frac{S_{12}'S_{14}'\Gamma_L}{1-\Gamma_L S_{11}'}\right|^2 \cdot |a_1|^2. \tag{11}$$

Also

$$b_1 = S_{11}'a_1 + S_{14}'a_4 = S_{11}'a_1 + S_{14}'b_4\Gamma_L.$$

Therefore

$$b_1 = S_{11}'a_1 + S_{14}'\Gamma_L \cdot \left\{\frac{S_{41}'a_1}{1-S_{44}'\Gamma_L}\right\} \tag{12}$$

$$\frac{b_1}{a_1} = \Gamma_{in} = S_{11}' + \frac{(S_{14}')^2\Gamma_L}{1-S_{11}'\Gamma_L}. \tag{13}$$

As shown in Fig. 14, the output power from each stage depends on the power into it, which in turn depends on its reflection coefficient. The calculation is therefore recursive, and the sequence is as follows.

1) Collect a separate parameter file for each of the N stages, consisting of

$$S1(k) = S_{11}' = S_{22}' = S_{33}' = S_{44}'$$
$$S2(k) = S_{21}' = S_{12}' = S_{34}' = S_{43}'$$

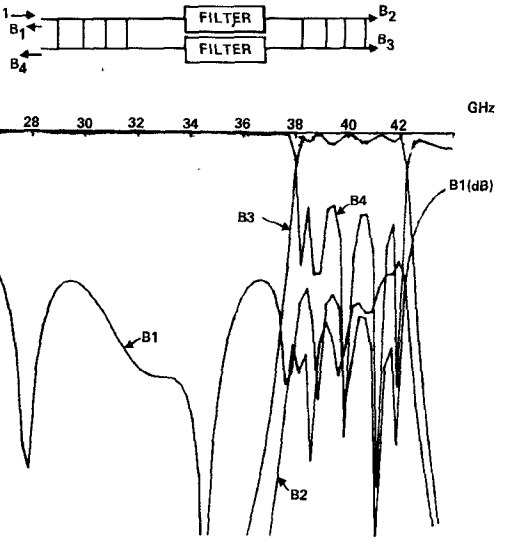

Fig. 15. Computed performance of one hybrid–filter–hybrid bandpass section.

$$S3(k) = S_{31}' = S_{13}' = S_{24}' = S_{42}'$$
$$S4(k) = S_{41}' = S_{14}' = S_{34}' = S_{43}' \qquad k = 1 \text{ to } N.$$

2) Starting with the stage (1) ($\Gamma(0) = 0$), with $\theta(k) =$ angular lengths between stages, from (13)

$$\Gamma(1) = S1(1)e^{-2j\theta(1)}$$

$$\Gamma(2) = \left\{S1(2) + \frac{S4(2)^2\Gamma(1)}{1-S1(2)\Gamma(1)}\right\} \cdot e^{-2j\theta(2)}$$

$$\vdots$$

$$\Gamma(k) = \left\{S1(k) + \frac{S4(k)^2\Gamma(k-1)}{1-S1(k)\Gamma(k-1)}\right\} \cdot e^{-2j\theta(k)}. \tag{14}$$

3) Knowing $\Gamma(k)$, calculate the output voltage of each stage starting with the input voltage (1) of the first stage, i.e., $a(N) = 1$, from (10).

$$a(k-1) = \frac{S4(k)\cdot a(k)}{1-S1(k)\cdot\Gamma(k-1)}, \qquad \text{for } k = N \text{ to } 2. \tag{15}$$

4) The output power of each stage is therefore from (11)

$$P(k) = \left|S3(k) + \frac{S2(k)S4(k)\Gamma(k-1)}{1-S1(k)\Gamma(k-1)}\right|^2 \cdot |a(k)|^2. \tag{16}$$

For the four-section multiplexer of Fig. 12, four data files are used to house the scattering parameters of each section. A section consists of identical bandpass filters connected by transmission lines between two 3-dB quadrature couplers. Because of symmetry the four-port scattering parameters can be determined from even- and odd-mode two-port analysis. The multiplexer utilizes 4 branch synchronous couplers and six-section 0.5-dB ripple Chebyschev filters.

A plot of scattered output power at the four-ports of one of the sections (3) is shown in Fig. 15. The main program brings up one section at a time starting with Section (1), furthest from the input. Each section input reflection coefficient $\Gamma(k)$ depends on the reflection coefficient of the following load, $\Gamma(k-1)$. Once all of the reflection coeffi-

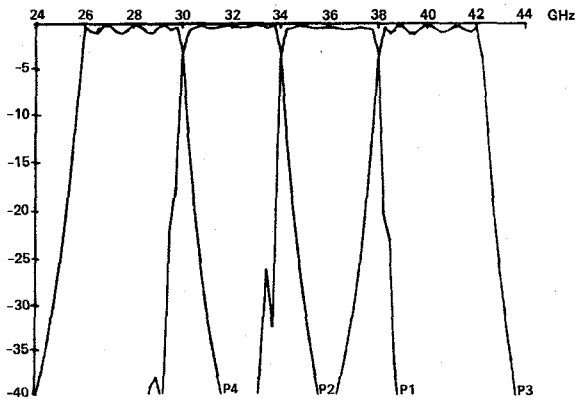

Fig. 16. Computed performance of integrated multiplexer.

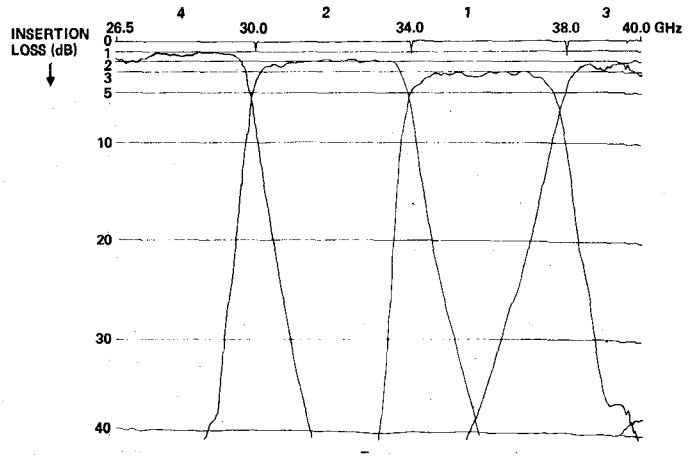

Fig. 17. Measured performance of NOSC *Ka*-band multiplexer.

cients are known the power output of each section follows from (15) and (16). Fig. 16 shows the results of the computer analysis. Circuit losses were not included. The actual circuit results of the NOSC quadruplexer are shown in Fig. 17.

VII. Conclusions

It has been shown how two-port analysis can be used to predict the behavior of complex circuits which contain symmetric four-ports. Multistage hybrid coupled amplifiers and frequency multiplexers were analyzed in this manner and compared to measured results.

A four-diode, two-stage, hybrid coupled InP Gunn amplifier was constructed with 5-dB gain over 33–37 GHz. The bandwidth was considerably less than that predicted by a computer model which did not account for waveguide to microstrip transitions. It was shown that VSWR effects at the input and output can severely degrade the performance of the amplifier much more than diode package parasitics or coupler directivity. Broad bandwidth hybrid coupled monolithic amplifiers are unlikely to perform well unless methods are developed for fabricating ferrite isolators on semi-insulating substrates.

With the exception of dissipative losses, which were not accounted for in the model, the computed and measured performance of the four-channel multiplexer were in close agreement. Computer analysis was mainly used to determine the interaction between multiplexer sections so that the individual filters could be designed for optimum bandwidth.

References

[1] H. J. Kuno and D. L. English, "Millimeter-wave IMPATT power amplifier combiner," *IEEE Trans. Microwave Theory Tech.*, vol. MTT-24, pp. 758–767, Nov. 1976.

[2] J. Reed and G. J. Wheeler, "A method of analysis of symmetrical four-port networks," *IRE Trans. Microwave Theory Tech.*, vol. MTT-4, pp. 246–252, Oct. 1956.

[3] J. K. Hunton, "Analysis of microwave measurement techniques by means of signal flow graphs," *IRE Trans. Microwave Theory Tech.*, vol. MTT-8, pp. 206–212, Mar. 1960.

[4] J. G. de Koning, R. E. Goldwasser, J. Hamilton, and F. E. Rosztoczy, "Gunn-effect amplifiers for microwave communication systems in *X*, *Ku*, and *Ka* bands," *IEEE Trans. Microwave Theory Tech.*, vol. MTT-23, pp. 367–374, Apr. 1976.

[5] D. Rubin, "Millimeter-wave microstrip amplifier using indium phosphide gunn diodes," in *1980 IEEE Int. Microwave Symp. Dig.*, pp. 67–69.

[6] R. Levy and L. F. Lind, "Synthesis of symmetrical branch-guide directional couplers," *IEEE Trans. Microwave Theory Tech.*, vol MTT-16, pp. 80–89, Feb. 1968.

[7] A. Hislop and D. Rubin, "Suspended substrate *Ka*-band multiplexer," *Microwave J.* pp. 73–77, June 1977.

David Rubin (M'70) was born in New York in November 1934. He passed his Amateur Radio license exam at age 12 and 1st Class Radiotelephone at age 17. After obtaining a B.A. in physics from the University of California, Berkeley, he worked briefly as an engineer at Edwards Air Force Base before fulfilling an Air Force ROTC commitment at a radar station in MI. After the Air Force assignment Mr. Rubin worked for three years at the Ford Scientific Laboratory in Dearborn, MI, simultaneously obtaining an M.A. in physics at Wayne State University.

Four more years were spent at the University of California, Riverside, where in 1966 Mr. Rubin was advanced to Ph.D. candidacy in physics, working in the area of nuclear and quadrupole resonance effects. A thesis was not completed. Instead, Mr. Rubin worked at the Naval Ordinance Laboratory in Corona, CA, for three years, transferring to the Naval Electronics Laboratory in San Diego, CA, (now the Naval Ocean Systems Center) where he has been employed since 1969. Early work in the Navy was associated with analog video matching techniques for use with radiometry, later microwave and millimeter-wave solid-state and microstrip circuits.

Mr. Rubin holds eight patents, two more pending. He has presented several papers at the IEEE International Microwave Symposia, and has authored several articles in the Microwave Journal and MTT-S Transactions. He was Chairman of the San Diego IEEE MTT-S group in 1974 and Chairman of the 1977 IEEE MTT-S International Microwave Symposium.